47th AIAA Aerospace Sciences Meeting Including The New Horizons Forum and Aerospace Exposition
5 - 8 January 2009, Orlando, Florida

AIAA 2009-382

A COMBINED EXPERIMENTAL-NUMERICAL STUDY OF THE ROLE OF WING FLEXIBILITY IN INSECT FLIGHT

Lingxiao Zheng, Xiaolin Wang, Afzal Khan, R. R. Vallance and Rajat Mittal[1]

Department of Mechanical & Aerospace Engineering, George Washington University, Washington DC 20052

Tyson L. Hedrick

Department of Biology, University of North-Carolina, Chapel Hill, NC 27599

ABSTRACT

An integrated program of research aimed at understanding wing flexibility and its implications for flight in insects is described. The experimental component of the research involves quantitative, high-speed videogrammetry of insects in free flight along with measurements of the mass and structural properties of the insect body and wings. The computational component of the research is centered on high-fidelity, flow and flow-structure interaction (FSI) modeling of insects in flight. The experiments provide data for the parameterization as well as the validation of the computational models.

INTRODUCTION

The wing is a key determinant of flight performance in insects. In the past few decades, insect flight mechanisms have been extensively studied theoretically, computationally and experimentally. The seminal work of Weis-Fogh (1956,1973) uncovered the "clap-and-fling" mechanism that is used by a number of insects and birds. Ellington (1996) drew attention to the importance of the leading-edge vortex as a key factor in lift generation by insects. More recently, Dickinson and coworkers (Dickinson and Gotz, 1996; Dickinson et al., 1999) identified delayed stall, rotational circulation and wake-capture as three distinct mechanisms that appear in experiments conducted with a dynamically scaled fruitfly wing. Wing-wing interaction in functionally four-winged insects such as dragonflies has also been studied by Mittal et al. (2006, 2008) and Wang et al. (2005).

All of the studies mentioned above have however assumed insect wings to be perfectly rigid. However, this is far from reality since wing flexibility and the associated deformation likely plays a significant role in insect flight (Wooton, 1981,1993), especially large insects such as moths, butterflies (as shown in Fig.1) and dragonflies. The potential that wing deformation leads to the generation of aerodynamic mechanism of lift/thrust production that are not possible with rigid wings has been hinted by a number of researchers (Combes et al., 2001; Lehmann, 2008; Sane, 2003; Wooton, 1993) but experiments or computational studies to date have found it hard to investigate this issue. Insects are difficult to visualize and model with a high level of detail because they are small, fast moving and flap their wings at high frequencies. Despite some recent quantitative visualization of insect in free flight (Sunada et al., 2002), the current literature lacks the necessary 3-D detail of body and wing kinematics needed for input into CFD analyses. As a result, no computational models of flapping flight have been validated with experimental data from freely flying insects. The effect of insect wing deformation and flexibility on the

---

[1] Professor; AIAA Associate Fellow; Corresponding author; mittal@gwu.edu

aerodynamics and flight performance has been even more difficult to quantify (Dudley, 2000). Prior investigations have attempted to quantify the 3D kinematics of insect flight, but did not achieve results with sufficient spatial and temporal resolution for use as inputs to CFD (Wilmott et al., 1997).
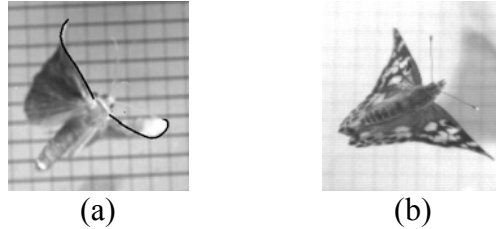

Figure 1. Various insect in flight showing wing flexibility. (a) Moth in climbing flight (b) Butterfly in flight.

In recent years, direct linear transformation (DLT) (Abdel-Aziz et al., 1971; Chen et al., 1994) and other photogrammetric techniques have been employed quite extensively in high-speed videogrammetry systems by Hedrick et al. (Hedrick et al., 2004 and 2007) and Lauder et al. (Lauder et al., 2006; Standen et al., 2005) for reconstructing fish swimming and avian flight kinematics respectively. However, it has not been applied to the study of the insect flight kinematics. In the current study, we experimentally measure 3-D kinematics (position, velocity and acceleration) for a grid of points on the surface of both the wings and body of free flying insects (butterflies) during different maneuvers (climbs, turns and hovers) with high-speed videogrammetry and DLT algorithm. This data is then used in to develop models for CFD analysis. The CFD solver is based on an existing Navier-Stokes immersed-boundary solver (Mittal et al., 2008) that has been developed to simulate complex biological flows.


METHODS AND PROCEDURES

The insects studied in this work are Painted Lady (*Vanessa Cardui*) and Monarch butterflies (*Danaus plexippus*) as well as a hawkmoth (*Manduca sexta*) shown in Figure 2. The insect flight videogrammetry setup used for the butterflies is shown in Figure 3. Butterflies are kept in a holding facility and transferred into glass chambers (chamber size varies according to the butterfly size) before the experiments. These butterflies fly inside the chambers which are illuminated by halogen photo optic lamps (OSRAM, 54428) with heat shields. Note that past studies have found that butterflies flying in enclosure maintain the allometry of their natural (unconstrained) flight (Dudley et al., 1994). Three, synchronized Photron FASTCAM 1024 PCI high-speed cameras with 1024×1024 pixel resolution, operated at 1000 Hz with at least 1/3000 sec. shutter speed are used to capture the butterfly free flight videos. Given that the butterflies flap at about 20Hz, this provides us with excellent temporal and spatial resolution of the butterflies in flight. The cameras are calibrated in three-dimensions using a portable calibration rig (shown in Figure 3) which is recorded at the end of each set of videogrammetry trial. The calibration rig was rapid prototyped with a precision of 0.25mm that allows accurate reconstruction of the positions of the body and wings during flight.
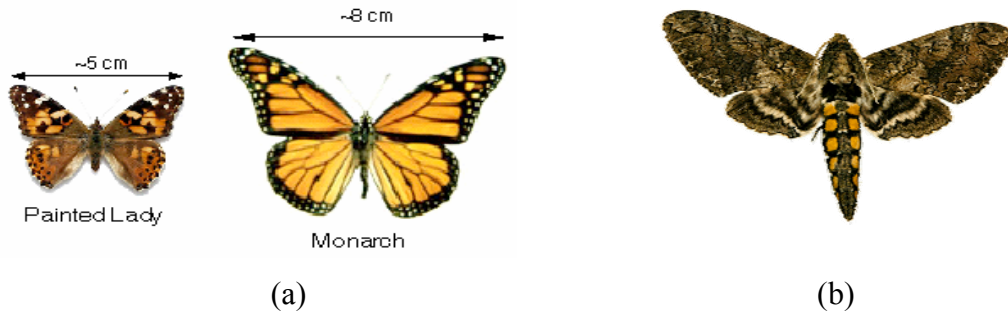
Figure 2. (a) Butterfly: Painted Lady and Monarch;   (b)   Hawkmoth: Manduca sexta (wingspan: ~11.2cm)

Various flight modes are elicited using fresh flowers, sugar water and other stimuli. The recorded sequences from the three cameras are downloaded continuously to a desktop computer for subsequent analysis. The video sequences are then examined and useable segments (segments where we get good quality visualization of 4-5 wing beats in level, climbing, hover or turning flight modes) identified for detailed DLT analysis. The objective of the DLT videogrammetry analysis is to determine with accuracy in time and space, the geometric conformation of the wings and body during flight. The individual body parts (wings, head, thorax, and abdomen) of the butterflies are weighed with a 0.01 mg accuracy balance (Ohaus™, Analytica Plus™). The wings are cut into about 25 pieces and each piece weighed individually to determine the center-of-mass and moment of inertia of the wings (note that total weight of a butterfly is about 150 mg).
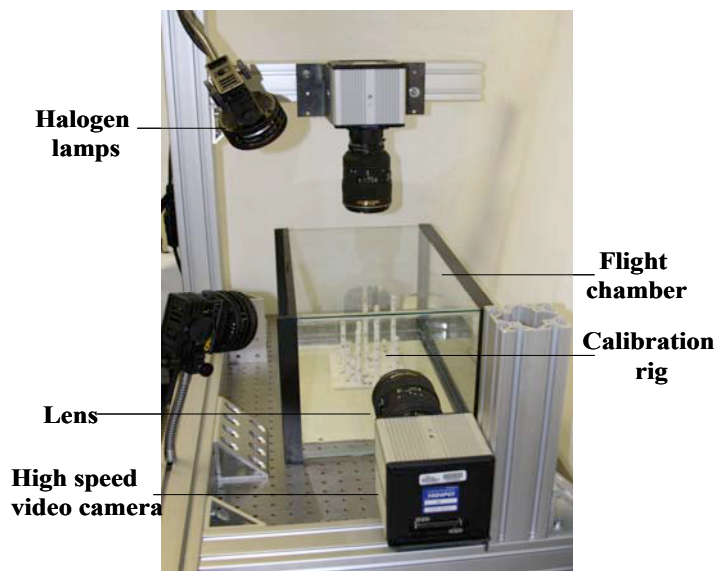

**Figure 3. High-speed insect flight videogrammetry setup.**

Natural markers on the butterfly wings and body are identified in image pairs and DLT is used to extract the 3D coordinates of these points at roughly 15 time-instants during each wing beat. An accurate representation of this butterfly in flight is constructed from the DLT analysis at each time instant. For development of the moth model we employ a slightly different technique. The study of the moth focused on hovering flight and here we use Autodesk® Maya® animation software to develop geometrical models of the wing during this flight mode.
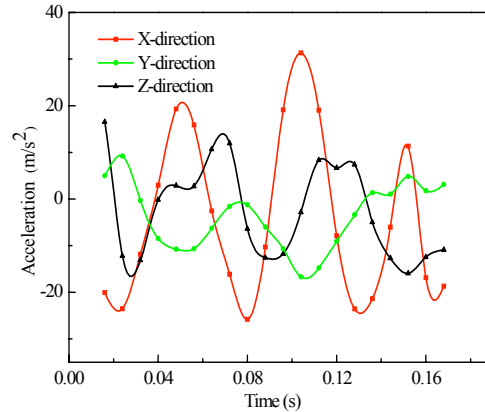
RESULTS

Butterfly Flight Experiments

Preliminary tests have been performed reconstructing the 3-D geometry and measuring the 3-D trajectory, velocity and acceleration of Painted Lady butterflies performing level and climbing flights. Figure 4 shows reconstruction of wing kinematics and flight trajectory of a butterfly performing level flight using high-speed videogrammetry. The four images (a-d) on the left are extracted from the same flapping cycle showing apparent wing deformation. The 3-D reconstructed body and wing coordinates are shown on the right. The trajectory of the butterfly is also obtained by tracking the position of the head via DLT and is shown in Fig. 4e. A critical component of these 3-D kinematic studies is the analysis of body acceleration. Determination of the mass distribution of insect body and wings and total body mass allows direct determination of net flight forces if whole body accelerations is measured accurately and inertial components of motion are accounted for. Determination of body acceleration together with knowledge of the mass distribution of the butterfly body allows a quantitative comparison of different maneuvers and provides data for the validation of forces calculated from the CFD models. Figure 4(f) shows experimental estimates of the acceleration of this butterfly obtained by tracking the position of the head. High levels of the instantaneous acceleration (up to 3g) are experienced by the butterfly, and similar high values have been reported in other studies (Sunada et al, 1993). Furthermore, the acceleration clearly allows us to determine the flapping frequency of the butterfly and is about 16Hz. The same procedure is used to obtain the 3-D kinematics of different points in the body and wings

4
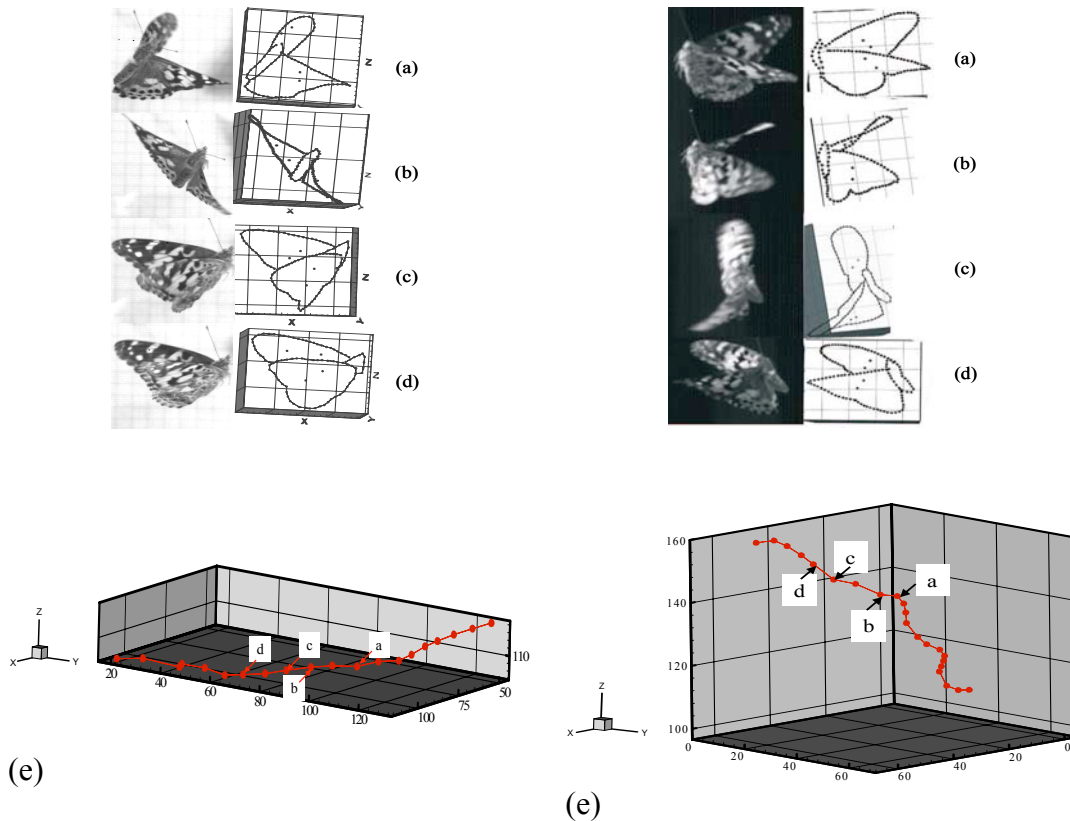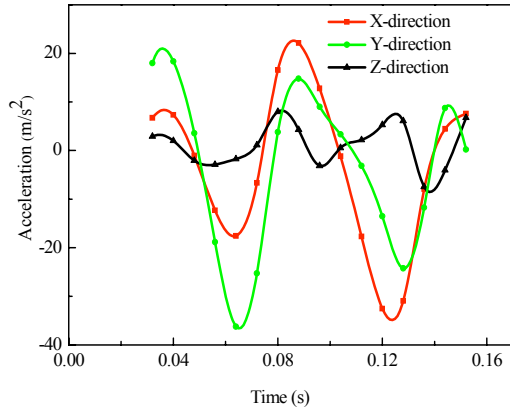
(f)   (f)

**Figure 4. Level flight**   **Figure 5. Climbing flight.**

Reconstruction of wing kinematics and flight trajectory of a Painted Lady butterfly using high-speed videogrammetry. (a-d) Frames from high-speed videos and reconstructed wing and body coordinates from videos using DLT. (e) Flight trajectory of the butterfly tracked using location of head. (f) Acceleration of body during flight.

Similarly, Fig. 5 shows reconstruction of wing kinematics and flight trajectory of a Painted Lady butterfly performing climbing flight. The four images (a-d) on the left are extracted from the same flapping cycle showing apparent wing deformation. The reconstructed body and wing coordinates are shown on the right. The trajectory of the butterfly is also obtained by tracking the head location via DLT study and shown in Figure 5(f). The acceleration of the butterfly is shown in Fig. 5(f) and this indicates that the flapping frequency of the butterfly is about 20Hz.

Computational Modeling of a Moth in Hover
The other insect model that is being developed is that of a Hawkmoth (*Manduca sexta*) in hover. This model is based on the experiments of Hedrick and Daniel (2006) who have obtained high-resolution videos of this insect hovering in front of an artificial flower. The geometry of the moth is constructed from a high-resolution (0.005" precision) NextEngine™ laser scanner of the body. Next, the 3D modeling, animation, visual effects, and rendering software Autodesk® Maya® is used to create a "animation" of the moth in flight where the wing kinematics are matched very closely to 16 different instances in the flapping cycle as observed in the high-speed video. This animation is then interpolated in time with a cubic spline to produce a high frame-rate animation suitable for input into the CFD solver. Figure 6 shows the animated geometric models at four time instants during the flapping cycle and it should be noted that we attempt to recreate the deformation observed in the wings.

Many past studies have examined hovering flight in hawkmoths (Ellington 1984; Den Berg, 1997; Hao Liu 1998, 2009). Some of these past studies have parameterized the wing motion in terms of time varying pitch, roll and stroke trajectory whereas others have used these types of parameterization to develop models for CFD analysis. The primary objective of the current study is to create the most high-fidelity CFD model of hovering flight in *Manduca* and then use this model to develop a comprehensive understanding of the aerodynamics of hovering insect flight. The long-term goal is to understand the role of wing flexibility on insect flight.
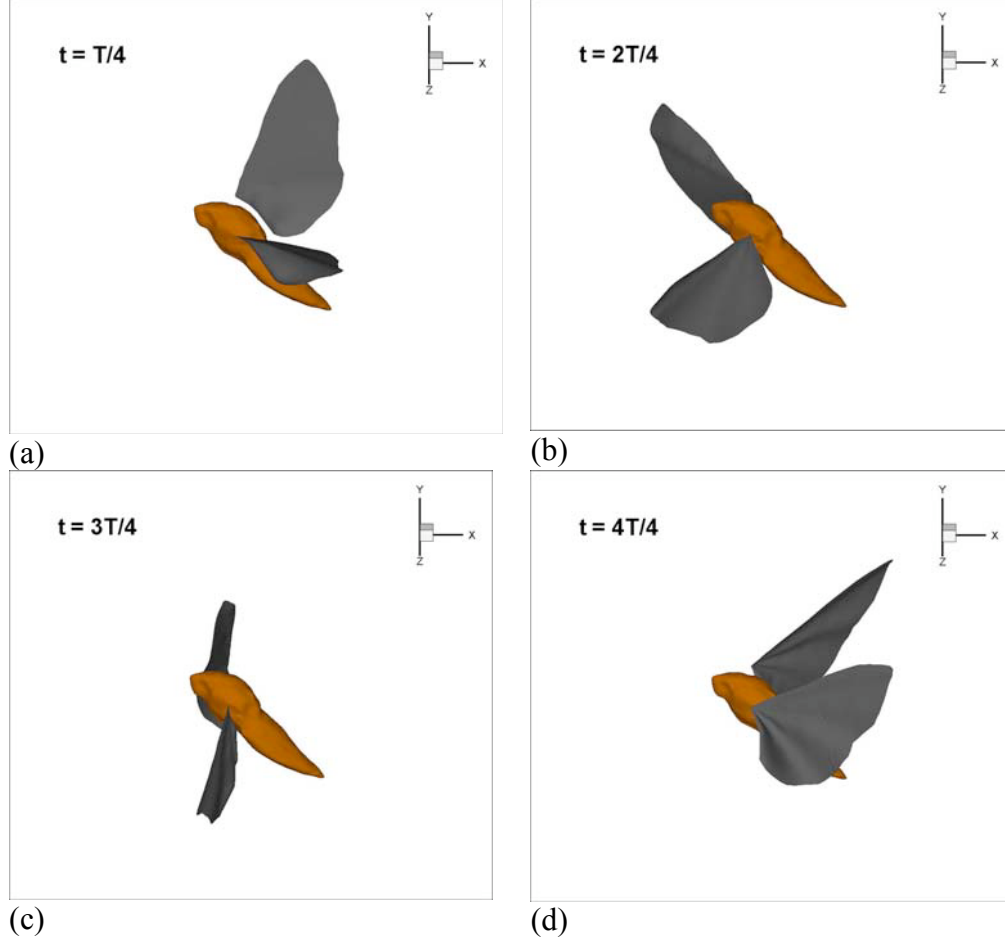
Figure 6. Four different phases in the flapping of the moth for the animated model constructed for CFD modeling.

Simulations have been carried out on a $128 \times 128 \times 128$ non-uniform Cartesian grid and four flapping cycles are simulated by which time, the flow has reached a stationary state. The Reynolds number for the flapping wings is defined as

$$\mathrm{Re} = \frac{U_{ref} L_{ref}}{v} = \frac{2\Phi f R c_m}{v},$$

where Φ is the angular wing beat amplitude, f is the flapping frequency, R is the wing length, c_m is the mean chord length, and v is the kinematic viscosity. For the insect under consideration, the Reynolds number is about 5350. Figure 7 shows the vortex structures produced from the simulations and a number of distinctive features can be observed. First, in Figure 7(b) we can clearly see the formation of spiral leading-edge vortices on both the wings during the downstroke. Also visible in the figure are a pair of tip vortices that extend backwards from the wing tips. During the upstroke, a number of vortices are shed from the wing into the hover jet that forms below the moth. It should be noted that the use of a non-dissipative central scheme for spatial discretization which does not employ any type of spurious dissipation allow the vortices to convect into the hover jet without excessive dissipation thereby allowing us to examine the vortex evolution in more detail.

Strong validation of the computed results is highly desirable. While detailed of the flow produced from the hovering moth have not been measured in the experiment, the forces generated by the insect can be indirectly determined from its motion and used for validation. Knowing the mass properties of wing, head, thorax and abdomen, it is possible to estimate the center-of-mass (CoM) of the moth and track this CoM. The acceleration of the CoM can then be determined by differentiating the displacement twice in time and the lift force generated by the wing extracted from this.

(a)

(b)

(c)

(d)

(e)

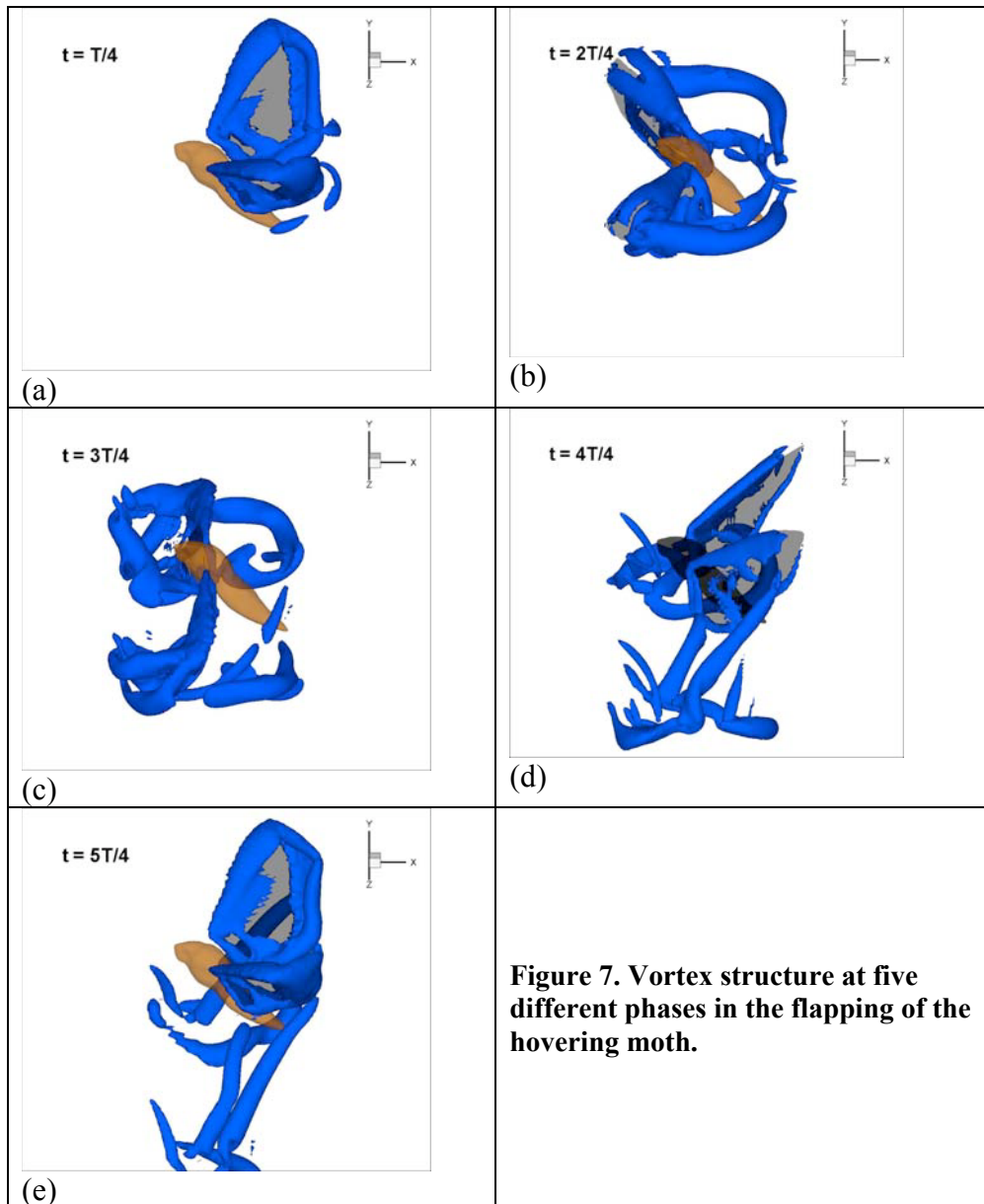**Figure 7. Vortex structure at five different phases in the flapping of the hovering moth.**

Figure 8 shows a comparison of the lift force computed via CFD with that estimated in the experiments and a number of interesting observations can be made from these. First, the mean value of computed lift is 15.0 mN which is quite close to the weight of the insect which is estimated to be about 13.7 mN. The comparison of the time variation also reveal that the peak lift force generated in the CFD model is about 40 mN and this matches well with the experimental

estimate also. In general, the force during the downstroke from the CFD is a reasonable match to that estimated from the experiments. The match during the upstroke is however not as good. First, there seems to be significant cycle-to-cycle variation in the upstroke lift force estimated from the experiments where as the CFD does not show similar variation since out model is based on cyclical repetition of the same flapping stroke. If one were to discount the cycle-to-cycle variation, we note the following similarities between the experiment and CFD: (1) both indicate that the upstroke produces lift which is significantly lower than that produced during the downstroke and (2) both show two local peaks in lift during the upstroke although the magnitudes and relative location of these peaks vary quite a bit in the experiment. The cause for this discrepancy is unclear. Clearly there are a number of uncertainties in both the CFD model as well as the experimental estimate which could cause these and these discrepancies are currently being explored further.
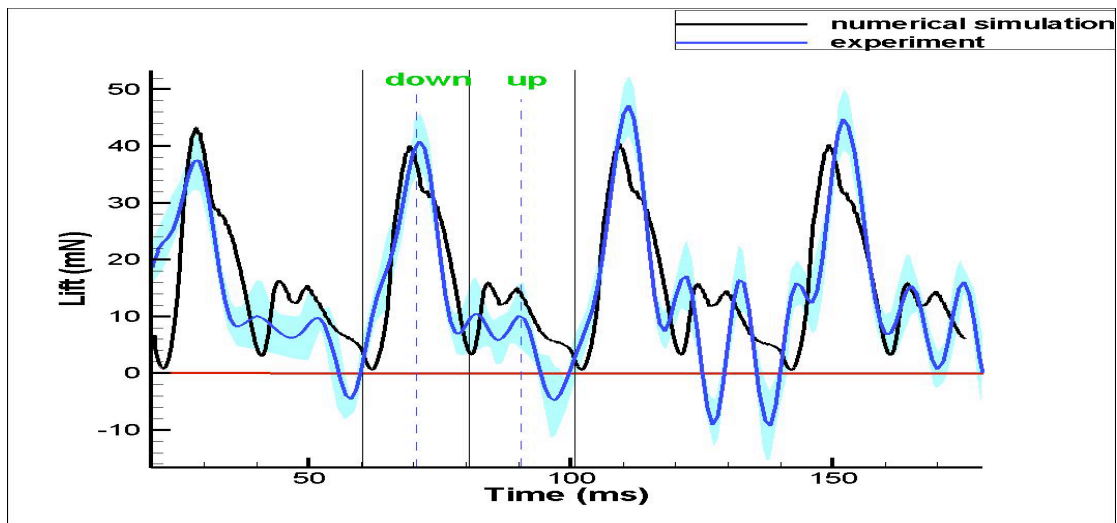

Figure 8. Comparison of lift force produced by CFD model and that estimated from the experiments.

ACKNOWLEDGEMENT

REFERENCES

Abdel-Aziz, YI and Karara, HM, Direct linear transformation from comparator coordinates into object space coordinates in close-range photogrammerty. *Proceedings of the Symposium on Close-Range Photogrammetry*, Falls Church, VA(1971).

Chen, L et al. , An investigation on the accuracy of the three-dimensional space reconstruction using the direct linear transformation. *J. Biomech.* 27: 493-500(1994).

Combes, SA and Daniel, TL, Shape, flapping and flexion: wing and fin design for forward flight. *J. Exp. Biol.* 204: 2073-2085(2001).

Coen Van Den Berg and Charles P. Ellington, The three-dimensional leading-edge vortex of a 'hovering' model hawkmoth. Phil. Trans. R. Soc. Lond. B 352 329-340(1997).

Dickinson, MH and Gotz, KG, The wake dynamics and flight forces of the fruit fly Drosophila melanogaster. *J. Exp. Biol.* 199: 2085-2104(1996).

Dickinson, MH et al., Wing rotation and the aerodynamic basis of insect flight. *Science* 284: 1954 - 1960(1999).

Dudley, R. *The Biomechanics of Insect Flight: Form, Function, Evolution. Princeton*. NJ: Princeton University Press(2000).

Dudley, R and Srygley, R, Flight physiology of neotropical butterflies: Allometry of airspeeds during natural free flight. *J. exp. Biol.* 191: 125-139(1994).

Ellington, CP, The aerodynamics of hovering insect flight. VI. Lift and power requirements. *Phil. Trans. R. Soc. Land B* 305, 115(1984).

Ellington, CP et al., Leading-edge vortices in insect flight. *Nature* 384: 626-630(1996).

Willmott, A. P. and C. P. Ellington, Measuring the angle of attack of beating insect wings: robust three-dimensional reconstruction from two-dimensional images. *Journal of Experimental Biology* 200(21): 2693-2704(1997).

Hao Liu, Integrated modeling of insect flight: from morphology, kenematics to aerodynamics. Journal of Computational Physics, Volume 228, Issue 2, 1February 2009: 439-459(2009).

Hedrick, TL et al., Wing inertia and whole-body acceleration: an analysis of instantaneous aerodynamic force production in cockatiels (*Nymphicus hallandicus*) flying across a range of speeds. *J. Exp. Biol.* 207: 1689-1702(2004).

Hedrick, TL and Daniel, TL, Flight control in the hawkmoth Manduca sexta: the inverse problem of hovering. *Journal of Experimental Biology* 209, 3114-3130(2006)

Hedrick, TL and Biewener, AA, Low speed maneuvering flight of the rose-breasted cockatoo (*Eolophus roseicapillus*). I. Kinematic and neuromuscular control of turning. E *J. Exp. Biol.* 210: 1897-1911(2007).

Johansson, LC and Lauder, GV, Hydrodynamics of surface swimming in leopard frogs (Rana pipiens) *J. Exp. Biol.* 207: 3945-3958(2004).

Lauder, GV et al., Locomotion with flexible propulsors: I. Experimental analysis of pectoral fin swimming in sunfish. *Bioinspiration & Biomimetics*, 1: s25-s34(2006).

Lehmann, F, When wings touch wakes: understanding locomotor force control by wake-wing interference in insect wings. *J. Exp. Biol.* 211: 224-233(2008).

Mittal, R et al., Computational Modeling and Analysis of Biomimetic Flight Mechanisms. AIAA 2002-0865(2002).

Mittal, R et al., An immersed-boundary method for flow-structure interaction in biological systems with application to phonation, *Journal of Computational Physics*, (2008.

Mittal, R. and Iaccarino, G., Immersed boundary methods. *Annual Review of Fluid Mechanics*, 37: 239-2612005).

Sane, SP, The aerodynamics of insect flight. *J. Exp. Biol.* 206, 4191-4208(2003).

Standen, EM and Lauder, GV, Dorsal and anal fin function in bluegill sunfish *Lepomis macrochirus*: three-dimensional kinematics during propulsion and maneuvering. *J. Exp. Biol.* 208, 2753-2763(2005).

Sunada, S et al., Performance of a butterfly in take-off flight. *J. Exp. Biol.* 183, 249-277(1993).

Sunada, S et al., Optical Measurement of the Deformation, motion, and Generated Force of the Wings of a Moth, *Mythimna Separata* (Walker) *JSEM International Journal B* 45: 836-842(2002).

Thomas, ALR et al., Force production and flow structure of the leading edge vortex on flapping wings at high and low Reynolds numbers. *Journal of Experimental Biology* 207: 4299-4323(2004).

Wang, H et al., Measuring wing kinematics, flight trajectory and body attitude during forward flight and runing maneuvers in dragonflies. *J. Exp. Biol.* 207: 745-757(2003).

Wang, J. K. and Sun, M., Unsteady aerodynamic force generation by a model fruit fly wing in flapping motion. *J. Exp. Biol.* 208: 3785-3804(2005).

Weis-Fogh, T., Biology and physics of locust flight. II. Flight performance of the desert locust (*Schistocerca gregaria*). *Phil. Trans. R. Soc. London. Ser B*. 239: 459-510(1956b).

Weis-Fogh, T., Quick Estimates of Flight Fitness in Hovering Animals, Including Novel Mechanisms for Lift Production. *J. Exp. Biol.* 59: 169-230(1973).

Wootton, RJ, Support and deformability in insect wings. *J. Zool., Lond.* 193: 447 -468(1981).

Wootton, RJ, Leading edge section and asymmetric twisting in the wings of flying butterflies (Insecta, Papilionoidea). *J. Exp. Biol.* 180: 105-117(1993).